Hot-working of advanced high-manganese austenitic steels

L.A. Dobrzański*, W. Borek

Institute of Engineering Materials and Biomaterials, Silesian University
of Technology, ul. Konarskiego 18a, 44-100 Gliwice, Poland
* Corresponding author: E-mail address: leszek.dobrzanski@polsl.pl

Abstract

Purpose: *The work consisted in investigation of newly elaborated high-manganese austenitic steels with Nb and Ti microadditions in variable conditions of hot-working.*

Design/methodology/approach: *The force-energetic parameters of hot-working were determined in continuous and multi-stage compression test performed in temperature range of 850 to 1100°C using the Gleeble 3800 thermomechanical simulator. Evaluation of processes controlling work-hardening were identified by microstructure observations of the specimens compresses to the various amount of deformation (4x0.29, 4x0.23 and 4x0.19). The microstructure evolution in successive stages of deformation was determined in metallographic investigations using light, scanning and electron microscopy as well as X-ray diffraction.*

Findings: *The investigated steels are characterized by high values of flow stresses from 230 to 450 MPa. The flow stresses are much higher in comparison with austenitic Cr-Ni and Cr-Mn steels and slightly higher compared to Fe-(15-25)Mn alloys. Increase of flow stress along with decrease of compression temperature is accompanied by translation of ε_{max} strain in the direction of higher deformation. Results of the multi-stage compression proved that applying the true strain 4x0.29 gives the possibility to refine the austenite microstructure as a result of dynamic recrystallization. In case of applying the lower deformations 4x0.23 and 4x0.19, the process controlling work hardening is dynamic recovery and a deciding influence on a gradual microstructure refinement has statical recrystallization. The steel 27Mn-4Si-2Al-Nb-Ti has austenite microstructure with annealing twins and some fraction of ε martensite plates in the initial state. After the grain refinement due to recrystallization, the steel is characterized by uniform structure of γ phase without ε martensite plates.*

Research limitations/implications: *To determine in detail the microstructure evolution during industrial rolling, the hot-working schedule should take into account real number of passes and higher strain rates.*

Practical implications: The obtained microstructure – hot-working relationships can be useful in the determination of power-force parameters of hot-rolling and to design a rolling schedule for high-manganese steel sheets with fine-grained austenitic structures.

Originality/value: The hot-deformation resistance and microstructure evolution in various conditions of hot-working for the new-developed high-manganese austenitic steels were investigated.

Keywords: High-manganese steel; Hot-working; TRIP/TWIP steels; Dynamic recrystallization; Static recrystallization; Grain refinement

1. Introduction

The beginning of XXI century has brought a development of new groups of steels to be applied for sheets in automotive industry. From the aspect of materials, this development has been accelerated by strong competition with non-metal aluminium and magnesium alloys as well as with composite polymers, which meaning is successively increasing. From the aspect of ecology, an essential factor it is to limit the amount of exhaust gas emitted into the environment. It's strictly connected to the fuel consumption, mainly dependant on car weight and its aerodynamics. Taking into consideration increased quantity of accessories used in modern cars, decreasing car's weight can be achieved solely by optimization of sections of sheets used for bearing and reinforcing elements as well as for body panelling parts of a car. Application of sheets with lower thickness preserving proper tautness requires using sheets with higher mechanical properties, however keeping adequate formability. Steels of IF and BH type with moderate mechanical properties and high susceptibility to deep drawing were elaborated for elements of body panelling [1]. The highest application possibilities belong to DP-type steels with ferritic – martensitic microstructure. Their mechanical properties can be formed in a wide range, controlling participation of martensite arranged in ferritic matrix. Sheets made of these steels are widely used for bearing and reinforcing elements [2].

In comparison to steels with ferritic microstructure they are characterized by high value of hardening exponent n, what decides about their strong strain hardening during sheet-metal forming [3].

Nowadays, apart from limiting fuel consumption, special pressure is placed on increasing safety of car's passengers. Constructional solutions and steels used in the frontal part of a vehicle are the most significant due to the possibility of accident occurrence. The goal of structural elements such as frontal frame side members, bumpers and the others is to take over the energy of an impact. Therefore, steels that are used for these parts should be characterized by high product of UTS and UEl, proving the ability of energy absorption. Among the wide variety of recently developed steels, high-manganese austenitic TRIP/TWIP steels with low stacking faulty energy (SFE) are particularly promising, especially when mechanical twinning occurs [3-6]. Beneficial combination of high strength and ductile properties of these steels depends on structural processes taking place during cold plastic deformation, which are a derivative of stacking fault energy (SFE) of austenite, dependent, in turn on the chemical composition of steel and deformation temperature [1-4, 7-10]. In case, when SFE is equal from 12 to 20 mJm^{-2}, partial transformation of austenite into martensite occurs, making use of TRIP effect (TRansformation Induced Plasticity) [1-4, 8]. Values of SFE from 20 to 60 mJm^{-2} determine intense mechanical twinning connected to TWIP effect (TWinning Induced Plasticity) [5-10]. The steels cover a very wide carbon concentration in a range from about 0.03 to 1 wt.%, 15-30% Mn, 0-4% Si, 0-8% Al.

The best conditions for obtaining the total elongation up to 80%, due to a gradual increase of mechanical twins, acting as obstacles for dislocation glide, occur when the carbon concentration is in the range of 0.4-0.8% and manganese from 17 to 22% [5, 11, 12]. However, high carbon content may lead to formation of M_3C and $M_{23}C_6$-type carbides, which precipitating on austenite grain boundaries negatively affect the strength and toughness of the steel [11]. Moreover, in the Fe-(17-22) Mn-(0.4-1) C steel grades, besides the formation of deformation twins during straining, a technologically undesirable jerky flow, which presents the features of dynamic strain aging and PLC (Portevin-LeChatelier) effect is observed [6]. Because of these reasons, Frommeyer et al. [1-4] proposed a group of high-manganese steels with carbon content, less than 0.1%. Lower hardening due to decreased carbon concentration was compensated by Si and Al additions, which together with Mn decide about SFE of the alloy and the main deformation mechanism. In a case of Mn ≥ 25%, the mechanical properties are mainly dependent on TWIP effect [1, 3, 13] and for Mn ≤ 20%, a process influencing a mechanical properties level is strain-induced martensitic transformation of austenite [2-4]. For

the latter the initial structure is consisted of γ phase as a matrix, some fraction of ε martensite and sometimes ferrite [2-4].

Results of our earlier investigations [14-17] indicate that ε martensite plates can appear in the initial structure of the (0.04-0.05) C-25Mn-4Si-2Al alloys as a result of Nb and Ti microadditions. The amount of C combined in precipitated carbonitrides reduces its content in the solid solution, thus decreasing the SFE of austenite and resulting in a presence of ε martensite despite high manganese concentration in the investigated steels. It was found [16-18] that the fraction of ε martensite plates is also dependent on a grain size of the γ phase and hot-working conditions. It was also observed that the fraction of mechanical twins within the austenite grains corresponds to the initial grain size, and at the same time affects the mechanical properties [5].

The hot-working behaviour of high-manganese steels is of primary importance for elaborating manufacturing methods consisted of hot rolling and successive cooling to room temperature. However, their hot work hardening and microstructural evolution controlled by thermally activated processes removing it, did not draw much attention compared to cold-working behaviour. Niewielski [19] compared the flow resistance of the 0.5C-17Mn-16Cr austenitic steel with conventional stainless steel of 18-8 type. He observed that the hardening intensity of Cr-Mn steel is much higher than in case of Cr-Ni steel. The difference in a course of work-hardening comes from a different ability of dislocations to splitting and association during straining.

High strain hardening rate is a result of the ability of manganese austenite for dislocation dissociation in the initial deformation stage [19, 20]. The reason for high hardening intensity of Cr-Mn steel are much higher flow stress values compared to Cr-Ni steel, however at lower deformation value of ε_{max} corresponding to maximal flow stress. For example, the yield stress of the Cr-Mn steel hot-twisted at a temperature of 1100°C with a strain rate of $1s^{-1}$ is equal to 134 MPa for the value $\varepsilon_{max} = 0.18$ and increases to 280 MPa for $\varepsilon_{max} = 0.23$ with decreasing the deformation temperature to 900°C [19]. Cabanas et al. [21] investigated the retarding effect of Mn content up to 20 wt.% on the grain boundary migration and dynamic recrystallization in binary Fe-Mn alloys. The influence of Al addition on the flow behaviour of 0.1C-25Mn-(0-8) Al alloys was the aim of investigations undertaken by Hamada et al. [22, 23]. They found that flow resistance is slightly higher for the 25Mn3Al than for the 25Mn steel. Moreover, they observed that the flow stress of the austenitic alloys containing Al up to 6% is much higher compared to the steel containing 8% Al with a duplex austenitic-ferritic structure [22].

Investigation results by Hamada et al. [22, 23], Sabet et al. [24] on 0.13C-29Mn-2.4Al steel and Kliber et al. [25] on (0.6-1)C-(17-20)Mn steels confirmed the high work hardening rate of high-manganese alloys in the deformation range lower than ε_{max}, likewise for Cr-Mn steels investigated by Niewielski [19].

For manufacturing methods elaborating, it is especially important that relatively low values of ε_{max} give the opportunities to refine austenitic structures in successive stages of hot-working. Unfortunately, the flow resistance of high-Mn steels is usually investigated under conditions of continuous compression or torsion [20-25]. To determine the softening kinetics, the double- or triple-deformation tests are rarely carried out [22, 25]. Hot-rolling of sheets consists of many passes characterized by the changing amount of deformation and strain rate from pass to pass. This means that the flow stresses should be determined during multi-stage straining testing and for various deformation values. In earlier investigations [14-16, 26, 27] we characterized the force-energetic parameters of hot-working of new-developed low-carbon high-Mn-Si-Al steels in continuous and four-stage compression tests. The aim of the paper is to describe in details the microstructure evolution and phase composition of 0.04C-27Mn-4Si-2Al-Nb-Ti steel subjected to four-stage compression with various amount of deformation.

2. Experimental procedure

Investigations were carried out on two high-manganese austenitic Mn-Si-Al steels containing Nb and Ti microadditions (Table 1). Melts were prepared in the Balzers VSG-50 vacuum induction furnace. After homogenization at 1200°C for 4 h to remove the segregation of Mn, ingots with a mass of 25 kg were submitted for open die forging on flats with a width of 220 mm and a thickness of 20 mm. Then, cylindrical machined samples $\varnothing$10x12 mm were made. In order to determine the influence of temperature on a steel grain growth, samples were solution heat-treated in water from the austenitizing temperature in a range from 900 to 1100°C (Fig. 1). Determination of processes controlling work hardening was carried out in continuous axisymetrical compression test using the DSI Gleeble 3800 thermomechanical simulator, used as laboratory equipment of the Institute for Ferrous Metallurgy in Gliwice [28, 29]. The stress – strain were defined in a temperature range from 850 to 1050°C with a strain rate of 10 s^{-1}.

In order to determine σ-ε curves, the four-stage compression tests were carried out. The temperatures of the successive deformations were 1100, 1050, 950 and 850°C. The details of

the hot-working are given in Table 2. To simulate various conditions of hot-rolling, the amount of true stain were 0.29, 0.23 and 0.19. The time of the isothermal holding of the specimens at a temperature of the last deformation was between 0 and 64 s. The specimens were inserted in a vacuum chamber, where they underwent resistance-heating. Tantalum foils were used to prevent from sticking and graphite foils used as a lubricant. The processes controlling the course of work-hardening were evaluated on a basis of the shape of σ-ε curves and structure observations of the specimens water-quenched on different stages of compression. To determine metallographically recrystallization progress at the interval between passes, a part of the specimen was water-cooled after isothermal holding of the specimens compressed at 900°C and 1000 °C with the amount of true strain of 0.29 and 0.5 and a strain rate of 10 s^{-1}.

Table 1. *Chemical composition of the investigated steels, mass fraction*

Designation	C	Mn	Si	Al	P	S	Nb	Ti	N
27Mn-4Si-2Al-Nb-Ti	0.040	27.5	4.18	1.96	0.002	0.017	0.033	0.009	0.0028
26Mn-3Si-3Al-Nb-Ti	0.065	26.0	3.08	2.87	0.004	0.013	0.034	0.009	0.0028

Table 2. *Parameters of the thermo-mechanical treatment carried out in the Gleeble simulator*

No	T_A, °C	Deformation I			Cooling I - II		Deformation II			Cooling II - III		Deformation III			Cooling III - IV		Deformation IV			$t_{isother}$ at 850°C, s	Final cooling
		T_1 °C	φ_1	$\dot{\varphi}_1$ s^{-1}	V_1 °C/s	t_1 s	T_2 °C	φ_2	$\dot{\varphi}_2$ s^{-1}	V_2 °C/s	t_2 s	T_3 °C	φ_3	$\dot{\varphi}_3$ s^{-1}	V_3 °C/s	t_3 s	T_4 °C	φ_4	$\dot{\varphi}_4$ s^{-1}		
1	1100	1100	0.29	7	5	10	1050	0.29	8	10	10	950	0.29	9	14	7	850	**0.29**	10	**0**	Water
2	1100	1100	0.29	7	5	10	1050	0.29	8	10	10	950	0.29	9	14	7	850	**0.29**	10	**4**	
3	1100	1100	0.29	7	5	10	1050	0.29	8	10	10	950	0.29	9	14	7	850	**0.29**	10	**16**	
4	1100	1100	0.29	7	5	10	1050	0.29	8	10	10	950	0.29	9	14	7	850	**0.29**	10	**32**	
5	1100	1100	0.29	7	5	10	1050	0.29	8	10	10	950	0.29	9	14	7	850	**0.29**	10	**64**	
6	1100	1100	0.29	7	5	10	1050	0.29	8	10	10	950	0.29	9	14	7	-	-	-	-	
7	1100	1100	0.23	7	5	10	1050	0.23	8	10	10	950	0.23	9	14	7	850	**0.23**	10	32	
8	1100	1100	0.19	7	5	10	1050	0.19	8	10	10	950	0.19	9	14	7	850	**0.19**	10	32	

T_A – austenitizing temperature, T_1...- T_4 – deformation temperatures, φ_1...- φ_4 – true strains, V_1...- V_4 – cooling rates between deformations, t_1...- t_3 – times between deformations, $t_{isother}$ – time of the isothermal holding of the specimens at a temperature of 850°C
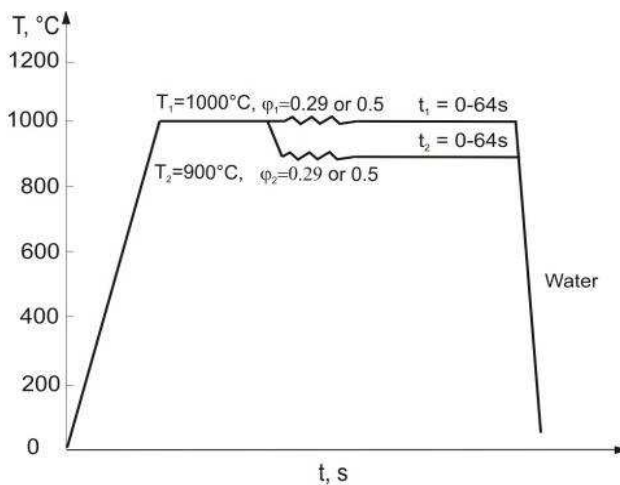
Figure 1. Parameters of the preliminary hot upsetting tests

Metallographic investigations were performed on LEICA MEF4A optical microscope. In order to reveal the austenitic structure, samples were etched in nitric and hydrochloric acids mixture in 2:1 proportion as well using a mixture of nitric acid, hydrochloric acid and water in 2:2:1 proportion. The structure of the investigated steel was also characterised using the SUPRA 25 scanning electron microscope and the JEOL JEM 3010 transmission electron microscope working at accelerating voltage of 300 kV. TEM observations were carried out on thin foils. The specimens were ground down to foils with a maximum thickness of 80 µm before 3 mm diameter discs were punched from the specimens. The disks were further thinned by ion milling method with the Precision Ion Polishing System (PIPS™), using the ion milling device (model 691) supplied by Gatan until one or more holes appeared. The ion milling was done with argon ions, accelerated by voltage of 15 kV.

3. Results and discussion

Melted steels possess diversified initial structure represented in Fig. 2 and Fig. 3. The new-developed 26Mn-3Si-3Al-Nb-Ti steel in the initial state is characterized by homogeneous microstructure of austenite with a grain size in range from 100 to 150 µm, in which numerous annealing twins can be identified (Fig. 2a). Single-phase microstructure of the steel is confirmed by X-ray diffraction pattern in Fig. 2b.
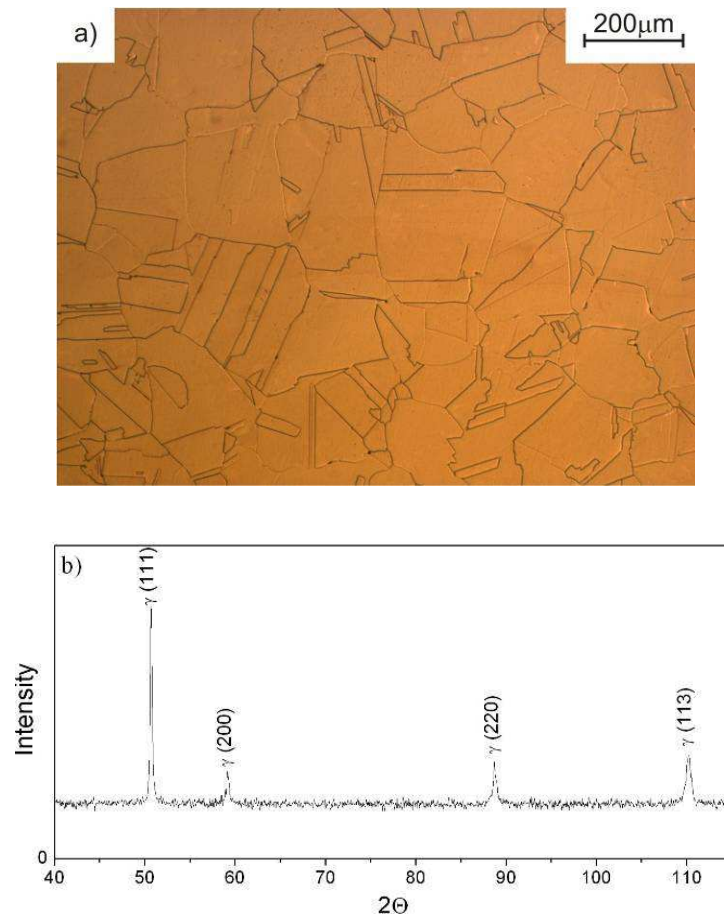
Figure 2. *Austenitic microstructure with numerous annealing twins of the 26Mn-3Si-3Al-Nb-Ti steel in the initial state (a) and X-ray diffraction pattern (b)*

The structure of the investigated 27Mn-4Si-2Al-Nb-Ti steel in the initial state after forging is shown in Fig. 3. Increased concentration of silicon up to 4% and its influence on the decreasing of the stacking fault energy of austenite result in the presence of some fraction of ε martensite in the austenite matrix containing many annealing twins. The ε martensite is present in a form of parallel plates inside austenite grains with a mean grain diameter of about 120 μm (Fig. 1b). The martensite plates are hampered by austenite grain or annealing twins boundaries. The presence of ε martensite is confirmed by X-ray diffraction pattern in Fig. 3b.
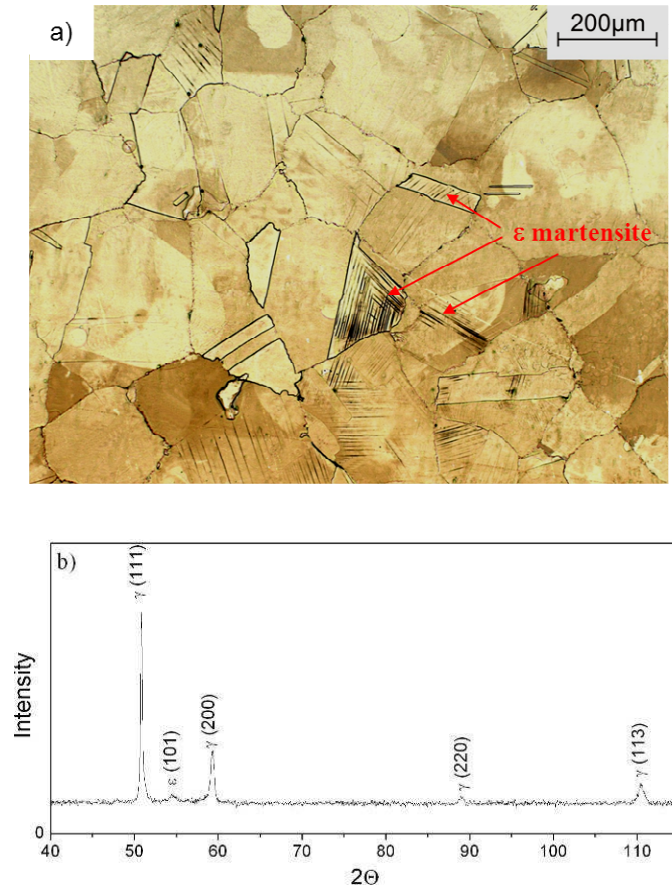
Figure 3. *X-ray diffraction pattern (b) and the austenite structure with many annealing twins and parallel ε martensite plates of the investigated steel 27Mn-4Si-2Al-Nb-Ti in the initial state (a)*

Starting point for microstructure analysis of specimens that were plastically hot-compressed in variable conditions are microstructures of steel subjected to solution heat treatment from a temperature range from 900 to 1100°C. The steel possesses fine-grained microstructure of austenite with grain sizes from 10 to about 17 µm up to temperature of 1000°C (Figs. 4a, b, c, Fig. 5). Further increase in solutioning temperature to 1100°C results in a rapid grain growth up to about 50 µm (Fig. 4c). This behaviour is connected with a total dissolution of NbC particles above 1000°C, what was investigated elsewhere [19]. Moreover, numerous annealing twins can be observed in the microstructure and some fraction of ε martensite plates (Fig. 4).
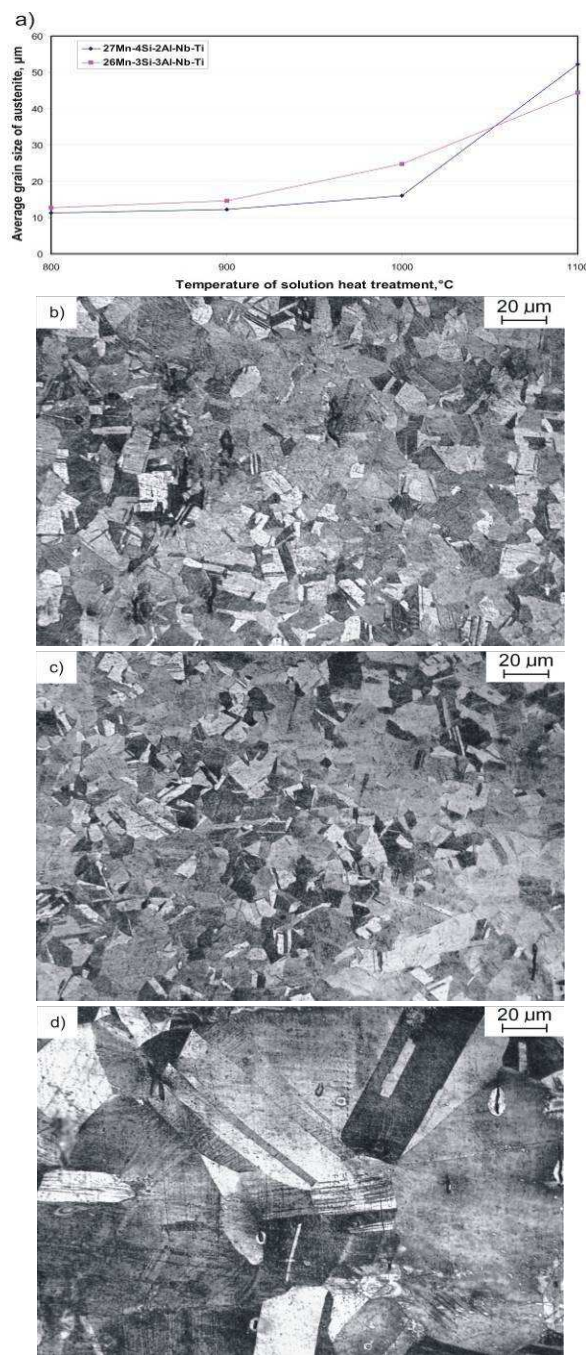
***Figure 4.** Changes of austenite grain size in dependence on temperature (a) and structures obtained after solution heat treatment from a temperature: b) 900°C, c) 1000°C, d) 1100°C; 27Mn-4Si-2Al-Nb-Ti steel*

Figure 5. *Austenitic structure of the 26Mn-3Si-3Al-Nb-Ti steel after solution heat treatment
from a temperature of 900°C*

Microstructure development of 27Mn-4Si-2Al-Nb-Ti steel, solution heat treated from temperature of 850 or 950°C, after application of specified reduction, as well as σ-ε curves obtained in continuous compression test are presented in Figs. 6a-h. It arises from Fig. 6a that the steel is characterized by values of yield stress equal from 240 to 450 MPa in investigated range of temperature. These values are considerably higher than they are for conventional C-Mn steels as well as for Cr-Ni and Cr-Mn austenitic steels [20].

It proves high strain hardening, which is probably caused by high Mn concentration in the steel. Additionally, the increase of flow stress is influenced by Si and Al additives as well as Nb and Ti microadditions. Decrease of strain temperature by around 100°C results in increase of flow stress by around 100 MPa. Along with strain temperature decreasing, the value of ε_{max} – corresponding to the maximum value of yield stress – is translating to a range of higher deformations. However, it's characteristic, that after strong strain hardening, peaks of ε_{max} are present for relatively low deformation values, i.e. from 0.23 to 0.48. It creates convenient conditions for using dynamic recrystallization for refinement of microstructure, what is confirmed by fine-grained microstructure of steel, solution heat treated from the temperature of 950°C after true strain of 0.5 (Fig. 6b). Decrease of true strain to 0.29, close to ε_{max} deformation in Fig. 6a, also leads to the initiation of dynamic recrystallization (Fig. 6c). Nevertheless, further decrease of reduction to 20% (true strain equal 0.23) is too low for initiating dynamic recrystallization (Fig. 6d). In such conditions, microstructure of steel is composed of dynamically recovered austenite grains elongated in the direction of plastic flow with size comparable to the sample solution heat treated from temperature of 900°C.
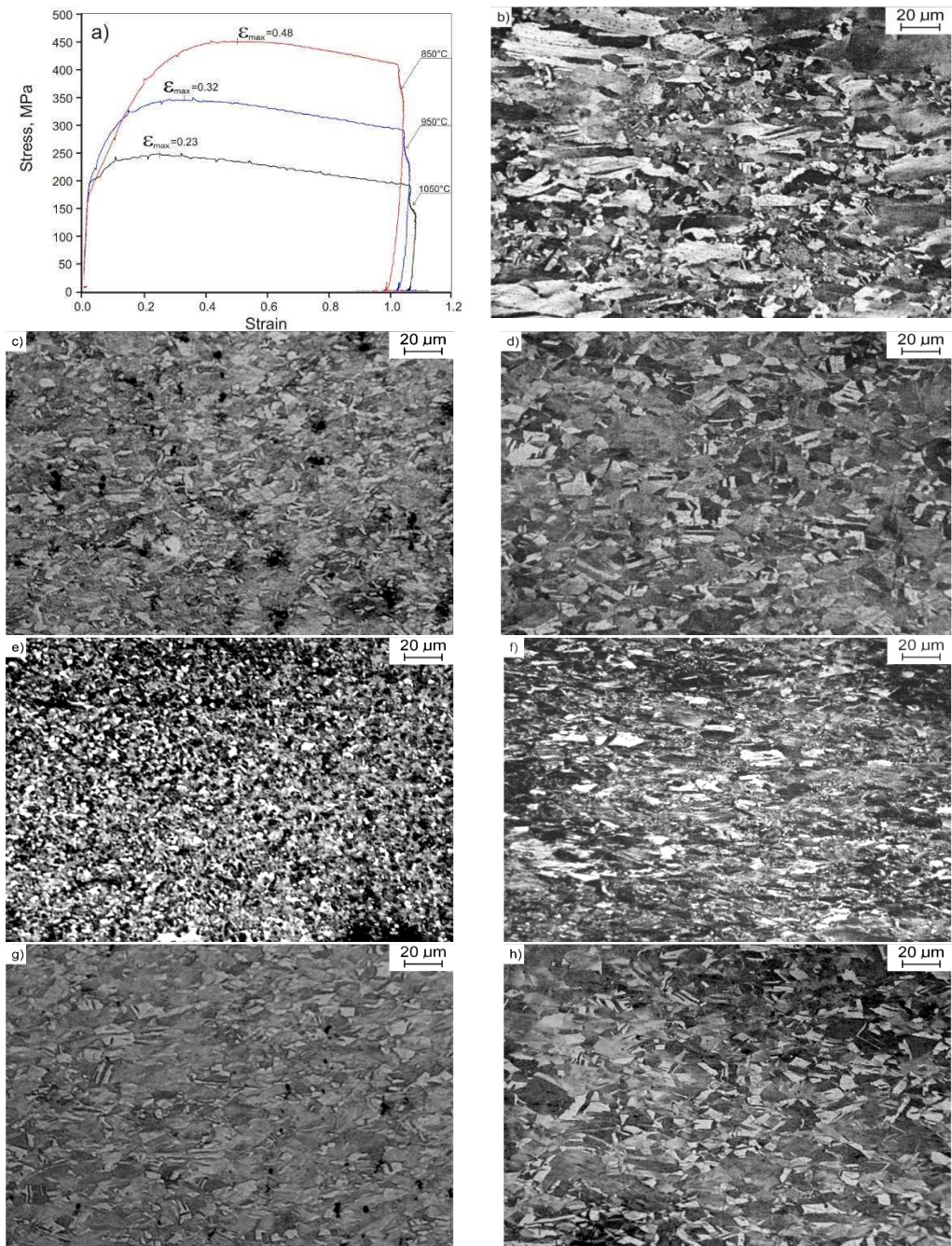
Figure 6. *Evolution of the microstructure of 27Mn-4Si-2Al-Nb-Ti steel compressed to a various strain: a)* σ-ε *curve; b) T = 950°C, ε = 0.5; c) T = 950°C, ε = 0.29; d) T = 950°C, ε = 0.23; e) T = 950°C, ε = 0.91; f) T = 850°C, ε = 0.5; g) T = 850°C, ε = 0.29; h) T = 850°C, ε = 0.23*

L.A. Dobrzański, W. Borek

After decreasing compression temperature to 850°C, fully recrystallized microstructure of austenite with grain size of approximately 3 µm was achieved through application of true strain equal 0.9 (Fig. 6e). Decrease of reduction to 40% results in obtaining microstructure of recrystallized grains of austenite uniformly distributed in matrix of dynamically recovered grains with sizes slightly smaller than for the strain temperature of 950°C (Fig. 6f). Decrease of true strain to 0.29 is sufficient for initiation of dynamic recrystallization also for the deformation temperature of 850°C (Fig. 6g), although the value of ε_{max} is equal 0.48. It's in accordance with data presented in [16], in which it was stated that the initiation of dynamic recrystallization can occur at critical deformation value $\varepsilon_{cd}=(0.5\text{-}0.85)\varepsilon_m$. Solution heat treatment from temperature of 850°C after true strain of 0.23 doesn't cause grain refinement of microstructure as a result of dynamic recrystallization. Microstructure of steel is composed of slightly deformed grains of dynamically recovered austenite (Fig. 6h).

The σ-ε curves together with microstructures of 26Mn-3Si-3Al-Nb-Ti steel solution heat treated from the temperature of 850°C and specified reduction are presented in Figs. 7a-d. The course of σ-ε curves is almost identical as in case of steel discussed above (Fig. 7a). It refers both to the values of flow stresses and values of ε_{max} deformations. It can be observed in Fig. 7a that the only difference derives from slightly lower values of flow stress for the strain temperature of 850°C, what can be caused by lower solution hardening of aluminium when compared to silicon, which concentration is twice smaller than in 26Mn-3Si-3Al-Nb-Ti steel. Similarly as for the second steel, true strain equal 0.23 is too low for initiating dynamic recrystallization (Fig. 7b), which occurs after increasing true strain to 0.29 (Fig. 7c). Still, significant microstructure refinement requires application of deformation equal 0.5 (Fig. 7d).

Development of microstructure of steel 26Mn-3Si-3Al-Nb-Ti isothermally held in temperature of 900°C, after true strain equal 0.29 is presented in Fig. 8. After 4 s of holding, microstructure is slightly different in comparison with microstructure of steel solution heat treated directly after deformation (Fig. 8a). Increase of holding time to 16 s results in obtaining high participation of recrystallized grains at the cost of dynamically recovered grains (Fig. 8b). Fast progress of microstructure reconstruction confirms occurrence of metadynamic recrystallization, not requiring any period of incubation. Confirmation of this fact is large portion of dynamically recrystallized grains after deformation with reduction of 25% at temperature of 850°C (Fig. 7c). Increase of holding time to 64 s leads to achievement of highly fine-grained microstructure of metadynamically and statically recrystallized grains (Fig. 8c).

Successive stages of microstructure development of steel 27Mn-4Si-2Al-Nb-Ti in function of isothermal holding time are shown in Fig. 9a-c. The progress of recrystallization of this steel

is slightly slower, what proves higher contribution of static recrystallization to removal of strain hardening than in case of steel 26Mn-3Si-3Al-Nb-Ti.
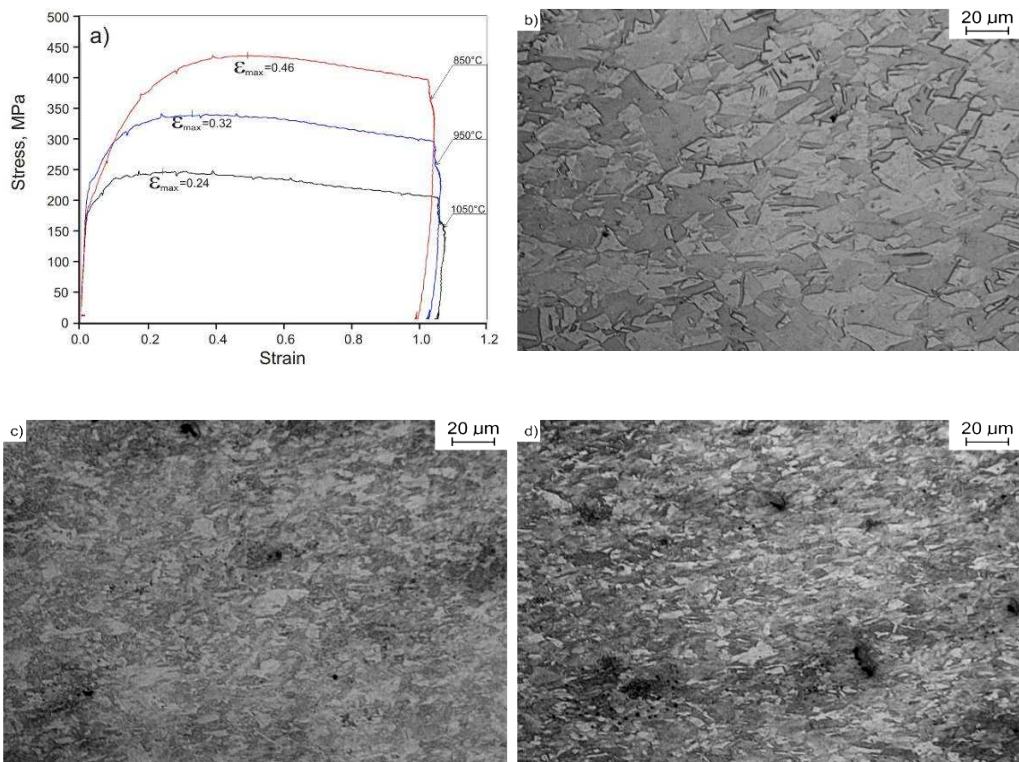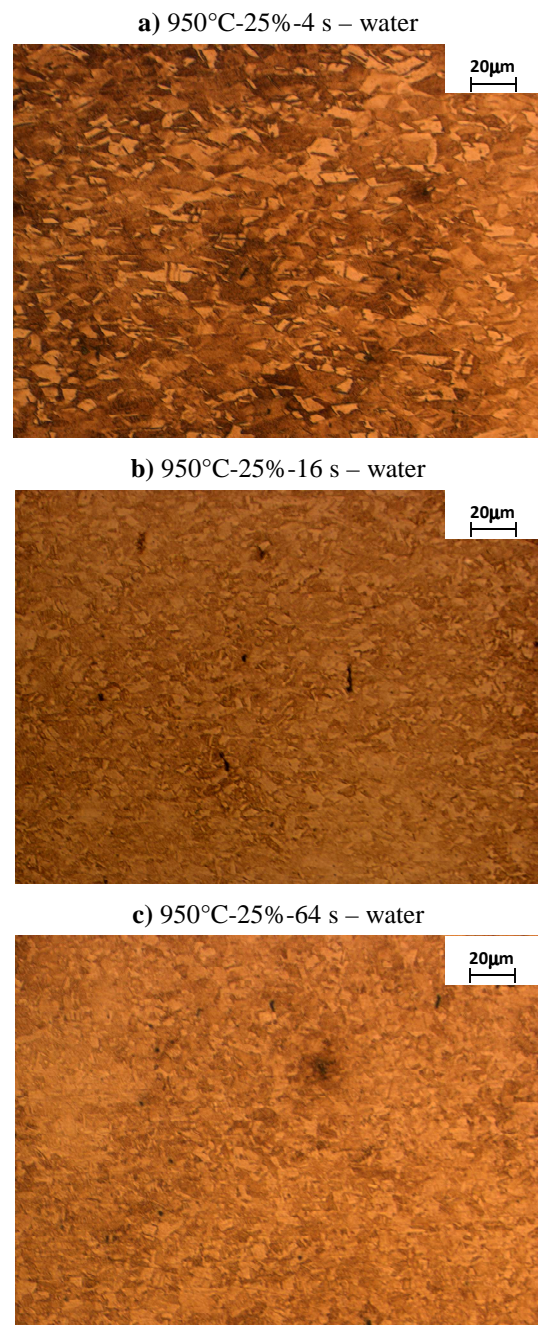

Figure 7. *Evolution of the microstructure of 26Mn-3Si-3Al-Nb-Ti steel compressed to a various strain: a) σ-εcurve; b) T = 850°C, ε = 0.23; c) T = 850°C, ε = 0.29; d) T = 850°C, ε = 0.5*

The conditions of hot-working additionally influence phase state of steel. Steel 26Mn-3Si-3Al-Nb-Ti with initial austenitic microstructure keeps its stability independently from conditions of plastic deformation. X-ray diffraction patterns for steel 27Mn-4Si-2Al-Nb-Ti indicate presence of peaks coming from ε martensite. However, their intensity connected with participation of this phase differs depending on applied variant of hot-working. The highest intensity from (101) planes belongs to the sample deformed with lowest reduction (Fig. 10a). Increase of reduction causes decrease of peaks intensity (Fig. 10b, 10c). Isothermal holding for 16 s after deformation at 900°C doesn't change phase composition of steel 27Mn-4Si-2Al-Nb-Ti. Still, slight peaks coming from ε martensite are present (Fig. 10d). Increase of holding time

to 64 s leads to substantial increase of (101) peak intensity of ε martensite (Fig. 10e). It means, that in spite of fine-grained microstructure of steel having impeding impact on growth of ε martensite laths [18], also state of internal stresses, effectively limited in process of metadynamic and static recrystallization, decides about tendency of formation of this phase in high-manganese steels.

The fraction of the recrystallized phase in intervals between successive passes can be evaluated from Figs. 11 and 12, showing a progress of recrystallization as a function of time for the specimens compressed in various deformation conditions. It arises from Fig. 11, that participation of recrystallized phase of 27Mn-4Si-2Al-Nb-Ti steel increases along with increasing deformation temperature and increase of reduction. Half-time of recrystallization at the temperature of 1000°C after deformation with 40% of reduction is equal 13 s and increases to 18 s after decreasing strain temperature to 900°C. Decrease of reduction to 25% results in elongation of $t_{0.5}$ time to 32 s, because of the change of prevailing participation of metadynamic recrystallization – in removing the effects of hardening – on behalf of static recrystallization. Half-times of recrystallization of 26Mn-3Si-3Al-Nb-Ti steel are shorter and are equal – 8, 12 and 17 s, respectively for analogical strain conditions (Fig. 12). It comes from higher participation of metadynamic recrystallization in removing effects of strain hardening, what arises directly from higher portion of dynamically recrystallized grains during plastic strain (Fig. 7c).

Stress-deformation curves of steels plastically deformed according to the parameters shown in Table 2 are presented in Figs. 13-15. Application of true strain equal 0.29 during cyclic compression creates possibility of the course of dynamic recrystallization, what is indicated by peaks that can be distinguished on σ-ε curves – especially for deformations realized at temperature of 1100 and 1050°C (Fig. 13). After decreasing plastic deformation temperature, maximum on σ-ε curves is present for maximum value of true strain (0.29). Initiation of dynamic recrystallization at this deformation value is additionally confirmed by microstructures of steels solution heat treated after deformation in analogical conditions of continuous compression (Figs. 6c, 6g, 7c). The values of yield stress in the range of strain temperature from 1100 to 950°C are comparable with values obtained in continuous compression test; however deformation of steel with lower concentration of Si and Mn requires slightly lower pressures. Significant decrease of flow stress is noted for the last deformation realized at the temperature of 850°C (Fig. 13). It's a result of partial removal of strain hardening through metadynamic recrystallization that occurs during the interval between third and fourth deformation. Additionally, cyclic deformation as well as the course of partial recrystallization result in much faster achievement of maximum on σ-ε curve for the fourth deformation when comparing to σ-ε curve of continuous compression at the temperature of 850°C.

a) 950°C-25%-4 s – water

**b)** 950°C-25%-16 s – water

c) 950°C-25%-64 s – water

Figure 8. *Microstructure evolution of the 26Mn-3Si-3Al-Nb-Ti steel after isothermal holding for time: a) t = 4 s; b) t = 16 s; c) t = 64 s; for the specimens plastically deformed at 900°C, ε = 0.29*

a) 950°C-25%-4 s - water

b) 950°C-25%-16 s - water

c) 950°C-25%-64 s - water
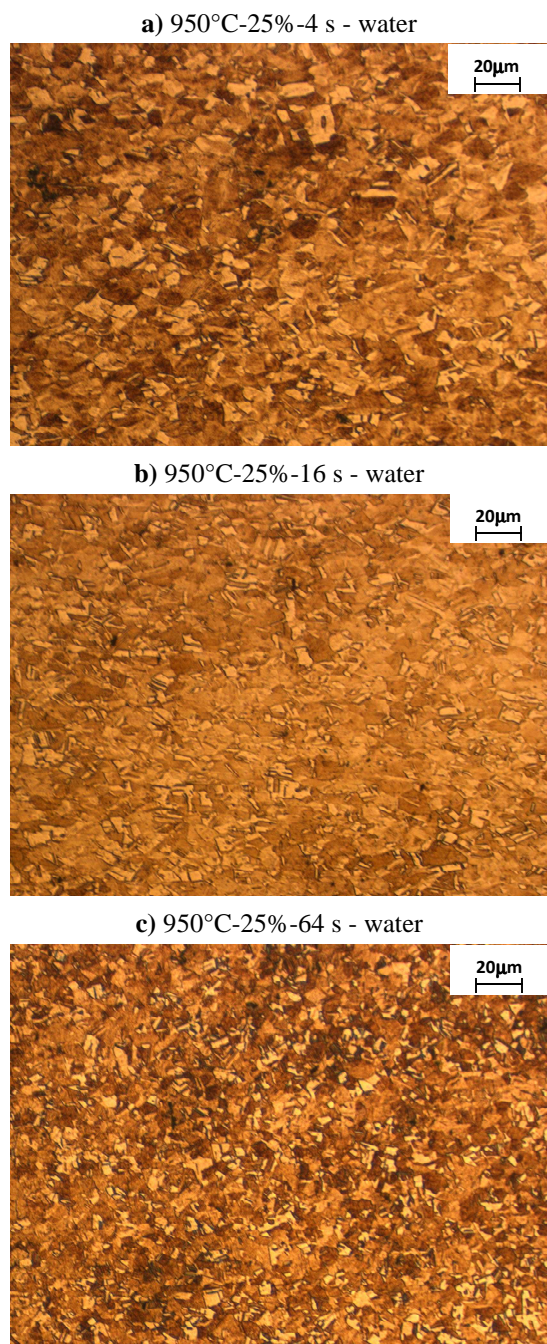
*Figure 9. Microstructure evolution of the 27Mn-4Si-2Al-Nb-Ti steel after isothermal holding
for time: a) t = 4 s; b) t = 16 s; c) t = 64 s; for the specimens plastically deformed at 900°C,
ε = 0.29*
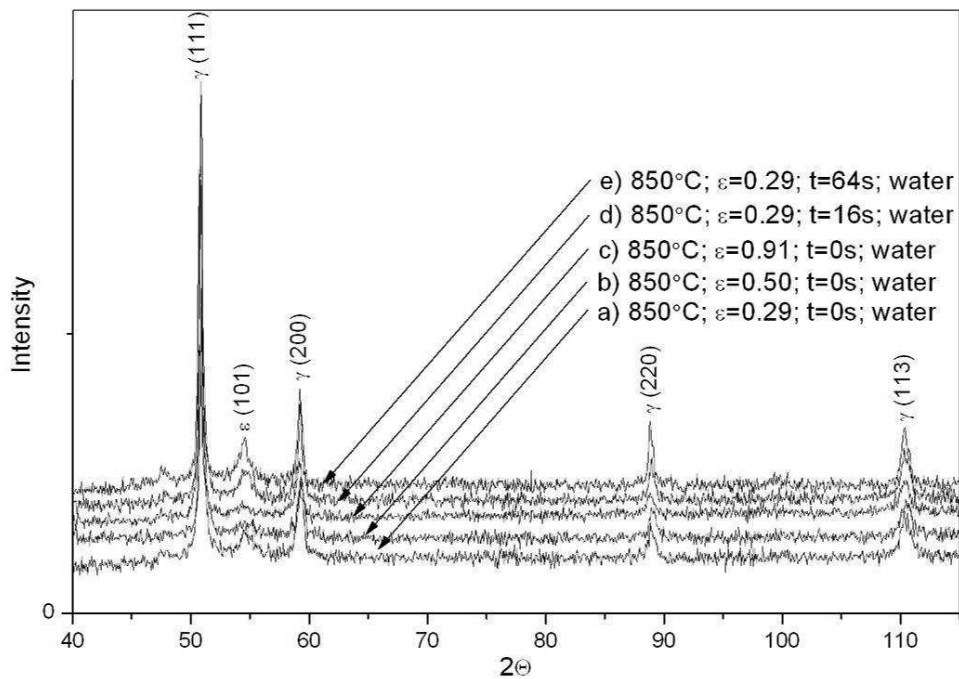
Figure 10. *X-ray diffraction patterns for 27Mn-4Si-2Al-Nb-Ti steel after various variants of the thermo-mechanical treatment; a) 850°C, $\varepsilon=0.29$, t=0 s, b) 850°C, $\varepsilon=0.5$, t=0 s, c) 850°C, $\varepsilon=0.91$, t=0 s, d) 850°C, $\varepsilon=0.29$, t=16 s, e) 850°C, $\varepsilon=0.29$, t=64 s*
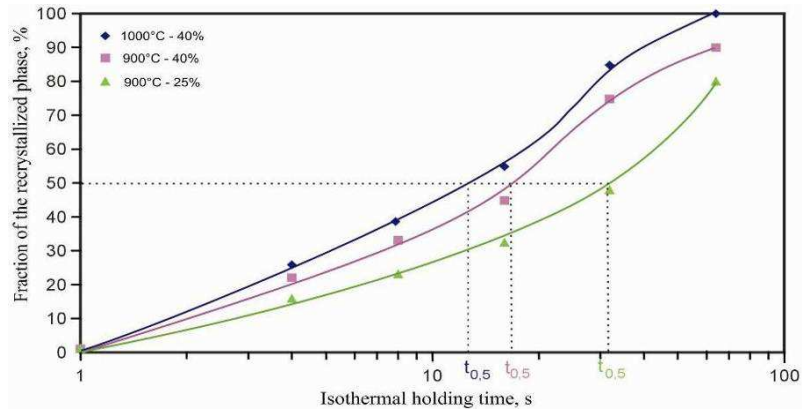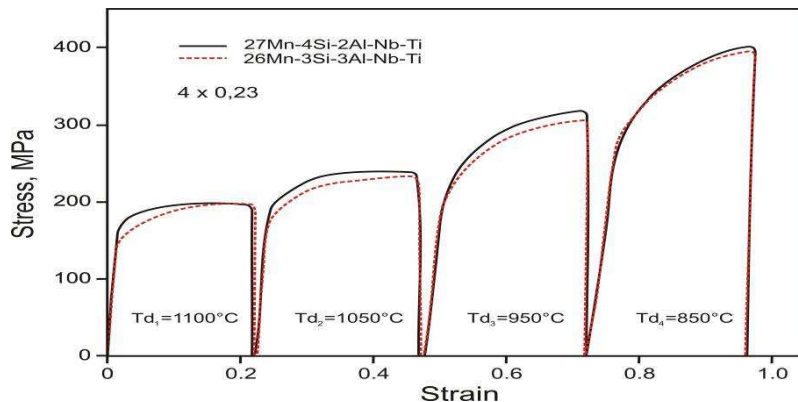

Figure 11. *Progress of recrystallization of the 27Mn-4Si-2Al-Nb-Ti steel isothermally held after plastic deformation in various conditions*
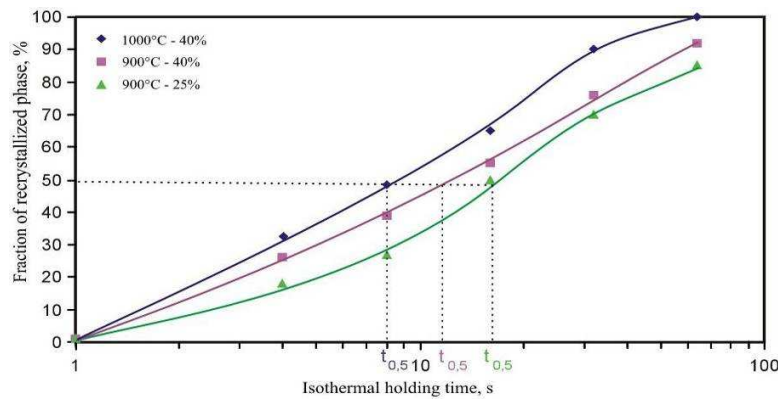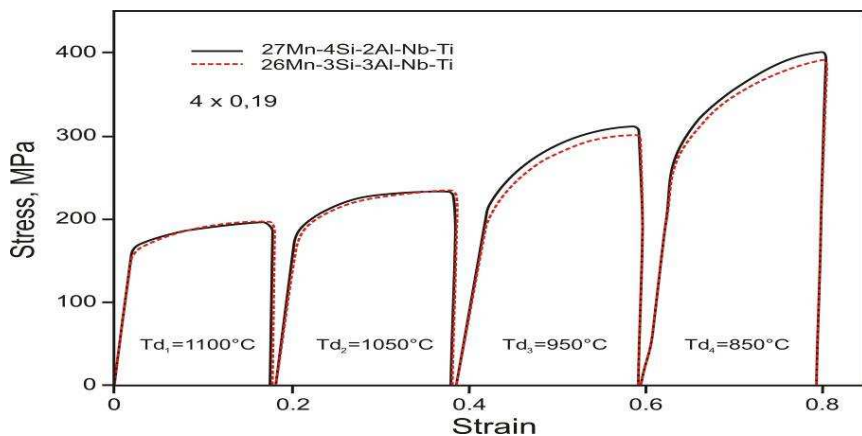
Figure 12. *Progress of recrystallization of the 26Mn-3Si-3Al-Nb-Ti steel isothermally held
after plastic deformation in various conditions*
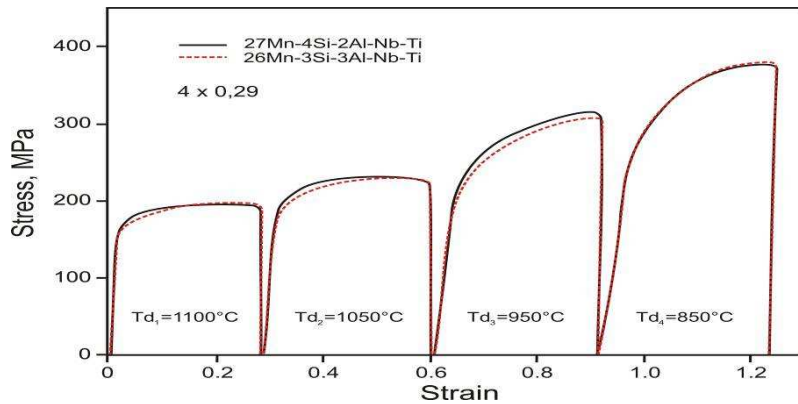
Figure 13. *Stress – strain curves for the specimens plastically deformed 4 x 0.29*
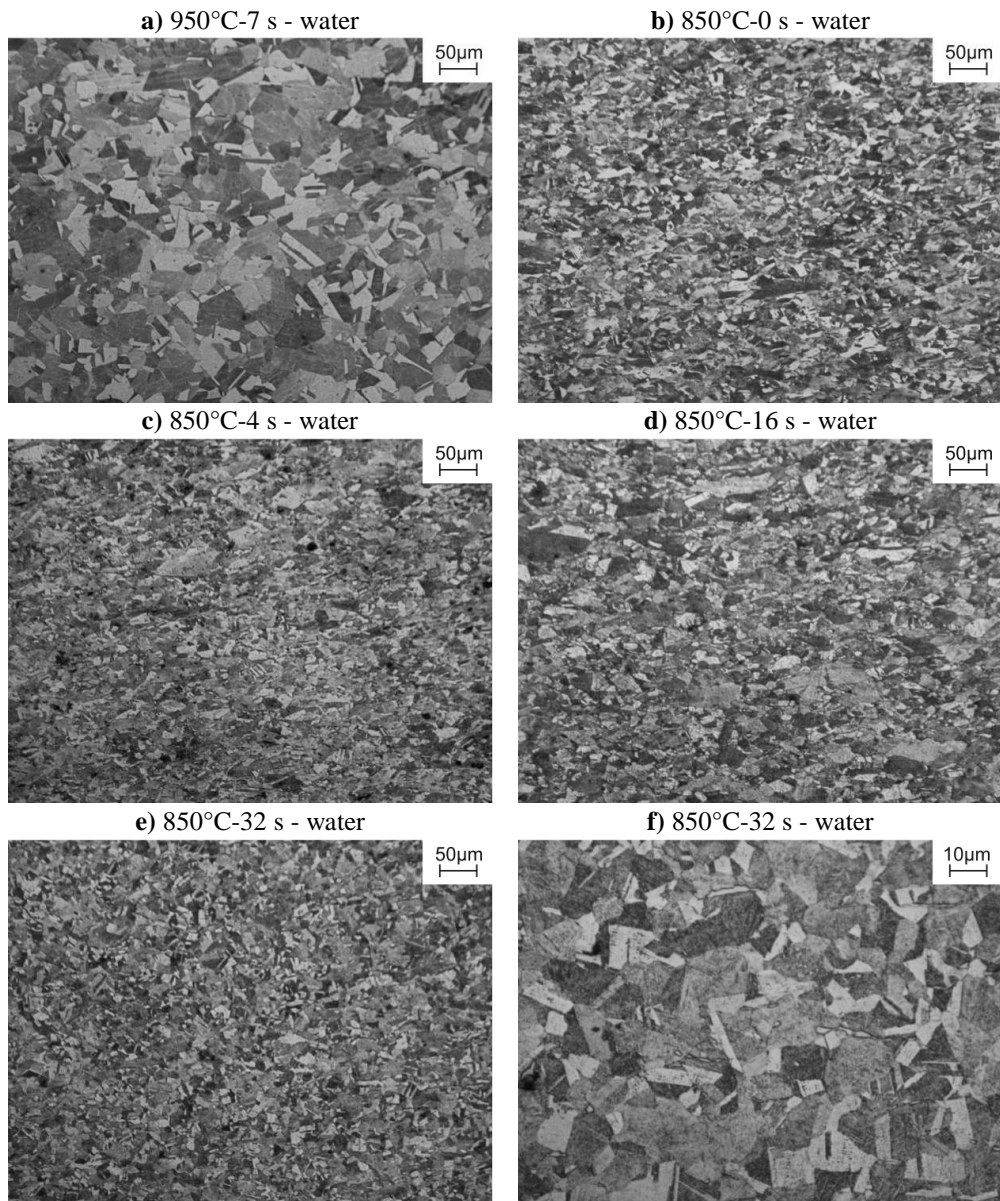

Figure 14. *Stress – strain curves for the specimens plastically deformed 4 x 0.23*

Figure 15. Stress – strain curves for the specimens plastically deformed 4 x 0.19

Decrease of true strain to 0.23 leads to a change of the course of σ-ε curves (Fig. 14). Shape of the curves after deformation at the temperature of 1100 and 1050°C indicate possibility of initiating dynamic recrystallization. However, decreasing the temperature causes that dynamic recovery is the process controlling strain hardening. Moreover, only partial course of static recrystallization during cooling of sample between third and fourth deformation results in increasing the value of yield stress during deformation at 850°C. Further decrease of true strain to 0.19 causes that dynamic recovery is the process controlling strain hardening in the whole temperature range of deformation (Fig. 15), at comparable values of yield stress.

The microstructure evolution of steel 27Mn-4Si-2Al-Nb-Ti in different stages of multi-stage compression is shown in Fig. 16. After deformation of the specimen at a temperature of 950°C and subsequent cooling for 7 s corresponding to the interpass time, the steel is characterised by uniform, metadynamically recrystallized austenite microstructure with a mean grain size of about 20 μm and many annealing twins (Fig. 16a). The initiation of dynamic recrystallization during the last deformation at the temperature of 850°C is confirmed by a micrograph in Fig. 16b, showing an initial state of dynamic recrystallization. The mean dynamically recovered austenite grain size decreased to about 12 μm and fine dynamically recrystallized grains are arranged along austenite grain boundaries as well as on twin boundaries. The similar role of twinning as a nucleation and growth mechanism of dynamic recrystallization was observed by Sabet et al. [24] in Fe-29Mn-2.4Al alloy. The repeated formation of twins during the whole temperature range of hot-working may be a reason of amplification of a number of dynamically recrystallized grains. The annealing twins are present both inside large dynamically recovered grains and fine recrystallized grains. A low tendency

a) 950°C-7 s - water

b) 850°C-0 s - water

c) 850°C-4 s - water

d) 850°C-16 s - water

e) 850°C-32 s - water

f) 850°C-32 s - water

Figure 16. Austenitic structures obtained after solutioning the steel 27Mn-4Si-2Al-Nb-Ti in successive stages of the hot-working for the specimens compressed to a true strain 4x0.29 and isothermally held for the time from 0 to 64s: a) metadynamically recrystallized grains during the interval between third and fourth deformation, b) initiation of dynamic recrystallization, c) grain refinement due to metadynamic recrystallization, d) grain refinement due to metadynamic and static recrystallization, e, f) fine statically recrystallized austenite grains

of high-manganese austenite with a low SFE to dynamic recovery is confirmed by Fig. 17, revealing a weakly outlined cellular dislocation structure in a region still not subjected to dynamic recrystallization, despite the true strain of 0.29, slightly higher than corresponding to a maximal value of true stress.

The analysis of Fig. 17 allows to reveal the highly deformed austenite structure with a various density of crystal structure defects, where inside, it is possible to observe regions with a much lower dislocation density corresponding to a state directly before forming dynamic recrystallization nuclei. A lack of distinct cellular dislocation structure in metals with low SFE is due to the necessity of extended dislocations to recombine it to a perfect dislocation before the cross slip initiation, what requires providing activation energy, dependent on normalized stacking fault energy of γ phase.
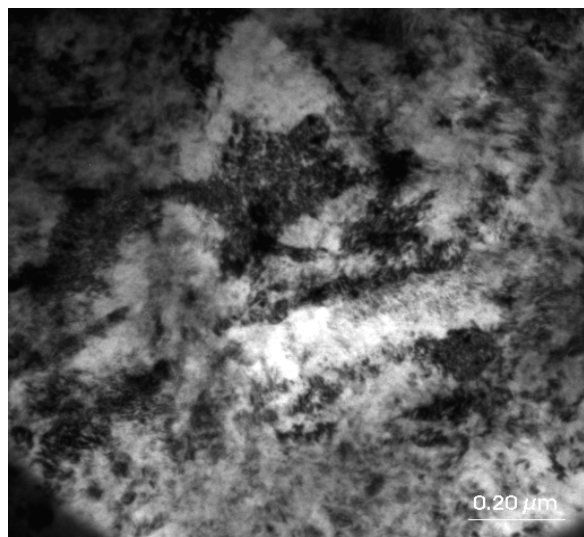

Figure 17. *Regions of dynamically recovered austenite with a various dislocation density of the steel 27Mn-4Si-2Al-Nb-Ti solution heat-treated from a temperature of 850°C directly after the true strain of 4x0.29*

Isothermal holding of the steel 27Mn-4Si-2Al-Nb-Ti after the deformation at 850°C for 4 s does not cause any essential modifications of microstructure. The microstructure consists of fine metadynamically recrystallized austenite grains and larger grains in which the process controlling the work hardening during deformation was just dynamic recovery (Fig. 16c).

Increase of isothermal holding of the specimen at a temperature of the last deformation for 16 s leads to growth of new grains as a result of metadynamic recrystallization and the initiation of static recrystallization on grain boundaries of large, flattened austenite grains whose fraction is still high (Fig. 16d). Further increase in the isothermal holding time to 32 s leads to obtain nearly 60% fraction of metadynamically and statically recrystallized microstructure with a mean austenite grain size of about 10 μm (Figs. 16e, f).

It is interesting that in Fig. 16 any ε martensite plates were observed, despite presence of this phase in the initial structure (Fig. 3). Confirmation of that fact is the X-ray diffraction patterns shown in Fig. 18 for different stages of thermo-mechanical treatment. A lack of ε martensite is connected with significant structure refinement compared to the initial state and hampering influence of grain boundaries on growth of ε martensite plates during cooling. Similar effects were reported in [18] for Fe-21Mn alloy and in [22] for Fe-25Mn alloy.
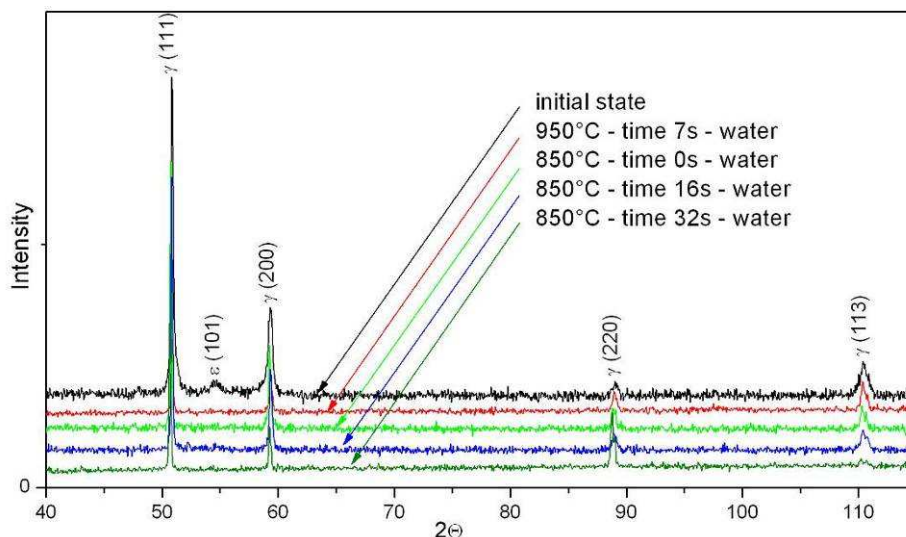
Figure 18. X-ray diffraction patterns of the steel 27Mn-4Si-2Al-Nb-Ti in the initial state and after different stages of thermo-mechanical treatment

Due to high rolling forces in final passes of sheet rolling, the amount of deformation is usually reduced. Because of this the four-stage compression with true strains of 4x0.23 and 4x0.19 were also carried out. Moreover, the applied strain is sufficient to initiate a course of dynamic recrystallization. However, decreasing the compression temperature to 950°C

causes that the flow stress is slightly higher and the applied strain value is too low to initiate dynamic recrystallization. Thus, process controlling a course of hot-working at 950°C is a dynamical recovery. Because of a lack of dynamic recrystallization in final passes, a refinement of microstructure requires the use of thermally activated, static processes removing work-hardening. For instance, the micrographs in Fig. 19 show the austenite microstructure of the steel isothermally held for 32 s at 850°C after compression with a true strain of 4x0.23. The fraction of statically recrystallized austenite equals approximately 60% (Fig. 19a). Numerous annealing twins can be observed in the microstructure (Fig. 19b) and a mean statically recrystallized austenite grain is higher compared to the specimen compressed 4x0.29, where a reconstruction of the microstructure was obtained both in static and metadynamic processes (Fig. 16f).

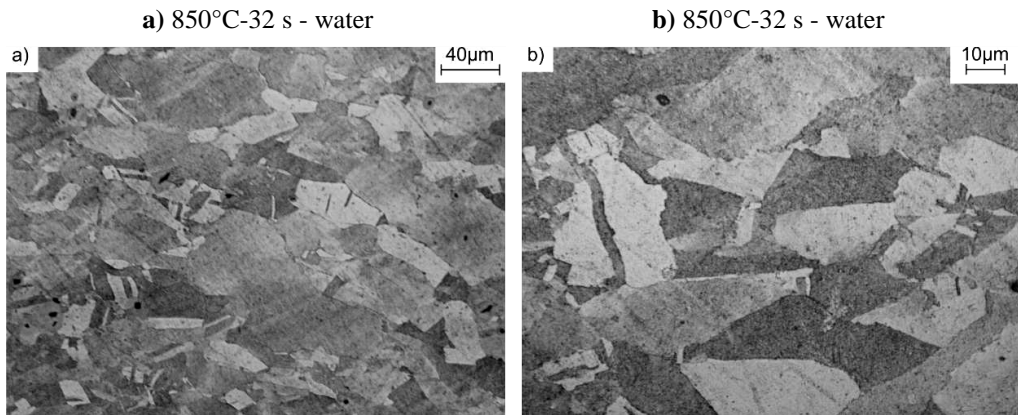**a)** 850°C-32 s - water   **b)** 850°C-32 s - water
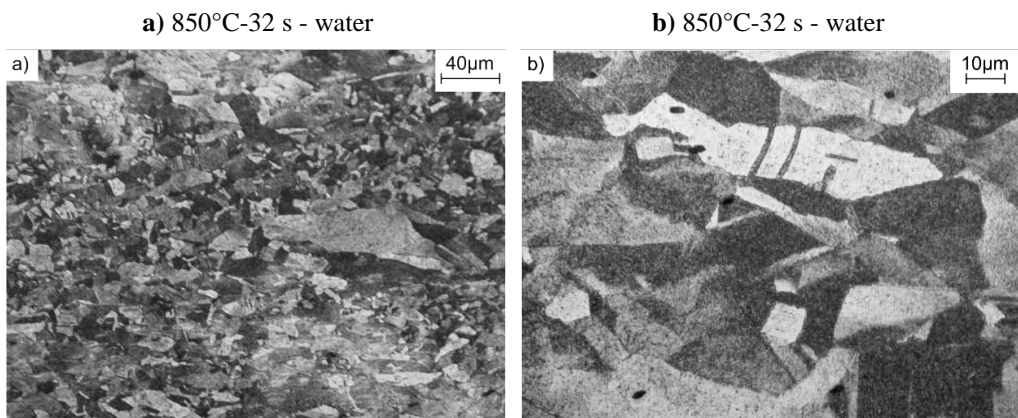
Figure 19. Fine, statically recrystallized austenite grains and large statically recovered grains of the steel 27Mn-4Si-2Al-Nb-Ti solution heat-treated from a temperature of 850°C after isothermal holding for 32 s of the specimen compressed with the true strain of 4x0.23 (a, b)

Relatively slow progress of static recrystallization is a result of impeding influence of high content of solutes on the migration of grain boundaries. The statically recovered, deformed austenite grains have low tendency to form a cellular dislocation structure, likewise dynamically recovered grains (Fig. 17). Inside these grains, regions characterized by various dislocation density can be observed (Fig. 20).
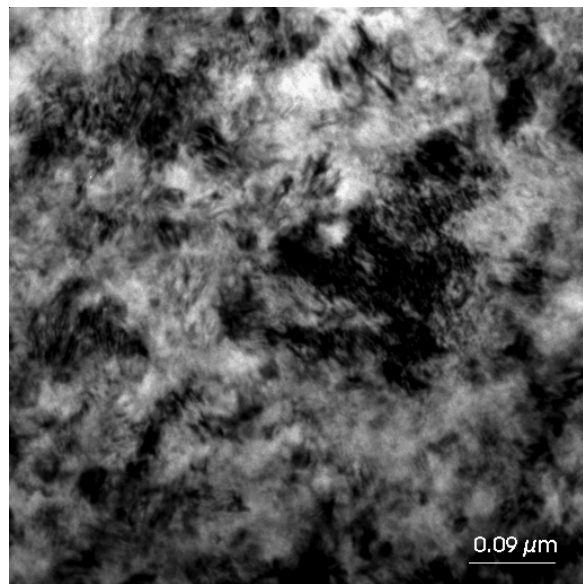
Figure 20. Regions of statically recovered austenite with a various dislocation density of the steel 27Mn-4Si-2Al-Nb-Ti solution heat-treated from the temperature of 850°C after isothermal holding for 32 s of the specimen compressed with the true strain of 4x0.23

a) 850°C-32 s - water   **b)** 850°C-32 s - water

Figure 21. Fine, statically recrystallized austenite grains and large statically recovered grains of the steel 27Mn-4Si-2Al-Nb-Ti solution heat-treated from the temperature of 850°C after isothermal holding for 32 s of the specimen compressed with the true strain of 4x0.19 (a, b)

A decrease of true strain to 0.19 causes that dynamic recovery is the process controlling strain hardening in the whole temperature range of deformation (Fig. 15), at similar values of flow stress in comparison with the specimen deformed 4x0.23. However, the isothermal holding of the specimen for 32 s is too short to obtain a desired fraction of recrystallized phase, which equals approximately 15% (Fig. 21a). Fine, recrystallized grains are located mainly on grain boundaries of large, flattened statically recovered grains (Fig. 21b). Both recrystallized and recovered grains are bigger than those after applying the true strain being equal 0.23 (Fig. 19). Once again, numerous annealing twins can be observed in the microstructure (Fig. 21a, b). The microstructure in Fig. 22 clearly shows that new grains are located on grain boundaries of large, statically recovered austenite grains. Moreover, a jerky-like character of the boundaries of large grains can be observed. It is a characteristic feature of a state directly before forming a recrystallization nucleus [19].
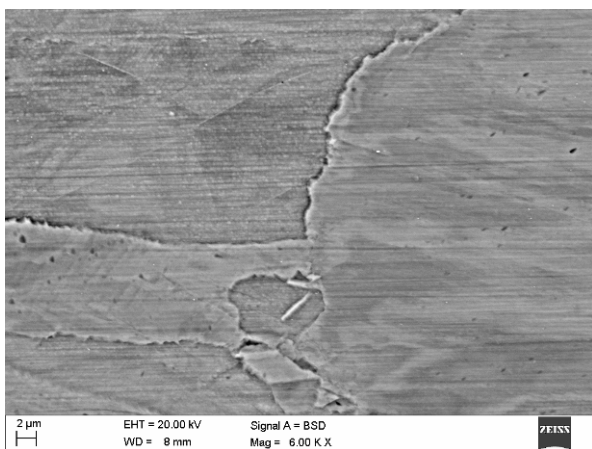
Figure 22. *The fine, statically recrystallized grain on jerky-like boundaries of three large, statically recovered grains of the steel 27Mn-4Si-2Al-Nb-Ti solution heat-treated from the temperature of 850°C after isothermal holding for 32 s of the specimen compressed with the true strain of 4x0.19*

Similarly microstructure evolution was observed for the specimens from 26Mn-3Si-3Al-Nb-Ti steel deformed in the multi-stage compression test. Microstructures of steel in the successive deformation stages and after its finish corresponding to σ-ε curves are put together in Fig. 23. After deformation of the specimen at a temperature of 1050°C and subsequent cooling for 10 s corresponding to the interpass time, the steel is characterized by uniform, metadynamically

recrystallized austenite microstructure with a grain size of about 40 μm (Fig. 23a). Lowering the deformation temperature to 950°C and the time of 7 s for cooling the specimen to 850°C results in much smaller fraction of metadynamically recrystallized grains located in a matrix of statically recovered grains (Fig. 23b). A partial removal of work-hardening through metadynamic recrystallization that occurs during the interval between third and fourth deformation is a result of significant decrease of flow stress noted for the last deformation realized at the temperature of 850°C (Fig. 13), compared to the curve obtained in the continuous compression test (Fig. 7a). Additionally, cyclic deformations as well as the course of partial recrystallization cause much faster achievement of maximum on σ-ε curve for the fourth deformation when comparing to continuous compression at the temperature of 850°C.

The initiation of dynamic recrystallization during the last deformation at a temperature of 850°C is confirmed by a micrograph in Fig. 23c, showing a partially recrystallized austenite with a grain size of about 20 μm. Isothermal holding of the specimen in a temperature of the last deformation for 16 s leads to a remarkably fine-grained metadynamically recrystallized austenite microstructure with a fraction of about 40%, located in the matrix of slightly elongated, statically recovered grains containing numerous annealing twins (Fig. 23d). Further extension of holding time to 32 s leads to obtaining almost fully recrystallized microstructure of steel (Fig. 23e) with a mean austenite grain size of about 10 μm. Holding of steel in the deformation temperature for 64 s causes gradual increase of recrystallized grains sizes (Fig. 23f).

Decrease of true strain to 0.23 during the multi-stage compression test leads to changes of the course of stress-strain curves (Fig. 14). A shape of the curves during deformation in a temperature range of 1100-1050°C and true stress values are comparable to that obtained after higher strain applying. Moreover, the applied strain is sufficient to initiate a course of dynamic recrystallization. However, decreasing the compression temperature to 950°C causes that the flow stress is slightly higher and the applied strain value is too low to initiate dynamic recrystallization. Thus, process controlling a course of hot-working at 950°C is a dynamical recovery.

Because of a lack of dynamic recrystallization in final passes, a refinement of microstructure requires the use of thermally activated, static processes removing work-hardening. For instance, the micrographs in Figs. 24a,b show the austenite microstructure of the steel isothermally held for 32 s at 850°C after compression with a true strain of 4x0.23. The fraction of statically recrystallized austenite equals approximately 50% (Fig. 24a). Numerous annealing twins can be observed in the microstructure (Fig. 24b) and a mean statically recrystallized austenite grain is higher compared to the specimen compressed 4x0.29, where a reconstruction of the microstructure was obtained both in static and metadynamic processes (Fig. 23e).

a) 1050°C-10 s - water

50µm

b) 950°C-7 s - water

50µm

c) 850°C-0 s -water

50µm

d) 850°C-16 s - water

50µm

e) 850°C-32 s - water

50µm

f) 850°C-64 s - water

50µm
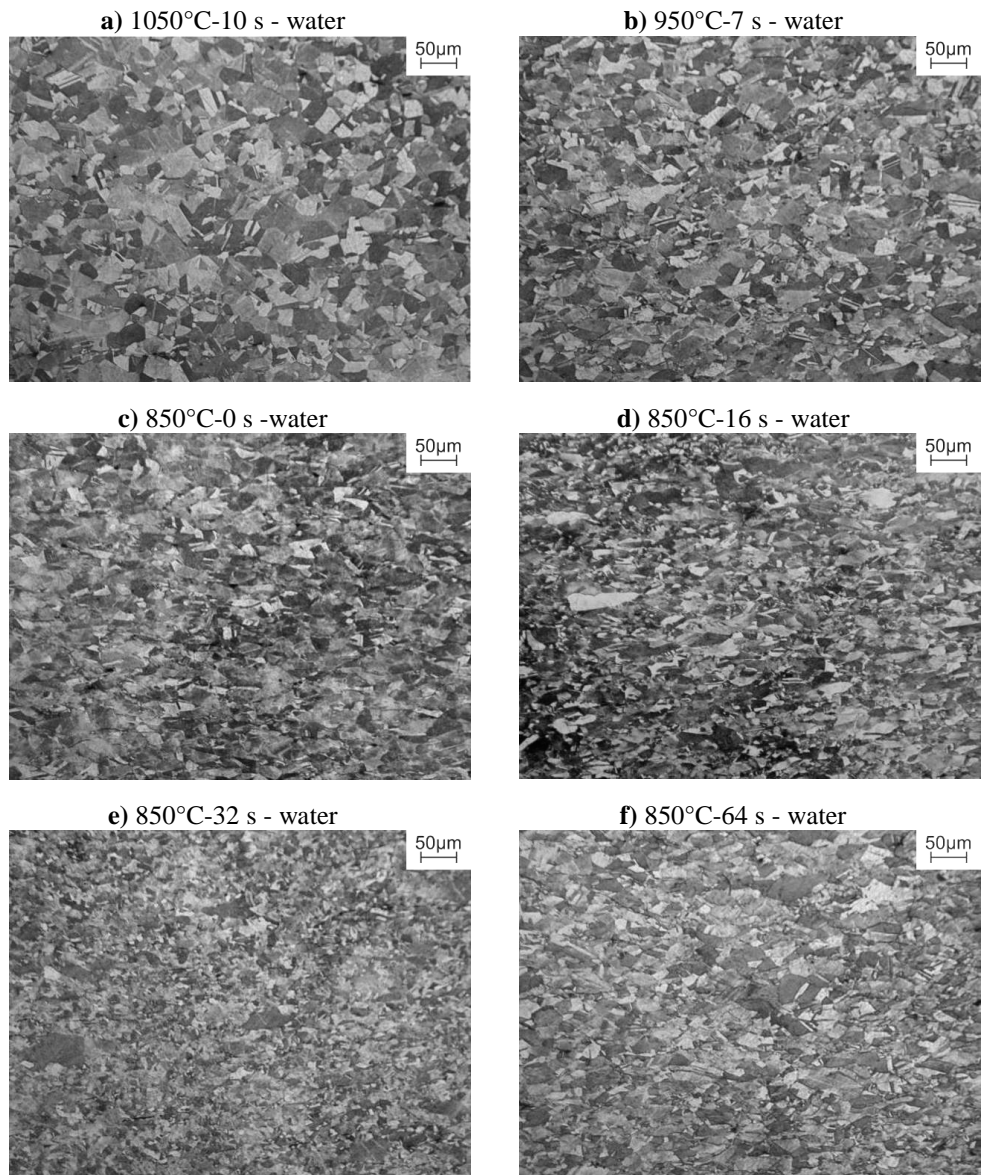
Figure 23. *Austenitic structures obtained after solutioning the 26Mn-3Si-3Al-Nb-Ti steel in successive stages of the hot-working for the specimens compressed to a true strain 4x0.29 and isothermally held for the time from 0 to 64s: a) metadynamically recrystallized grains during the interval between second and third deformation, b) metadynamically recrystallized grains during the interval between third and fourth deformation, c) initiation of dynamic recrystallization, d) grain refinement due to metadynamic and static recrystallization, e) fine statically recrystallized austenite grains, f) grain growth as a result of metadynamic recrystallization*

a) 850°C-32 s - water   **b)** 850°C-32 s - water
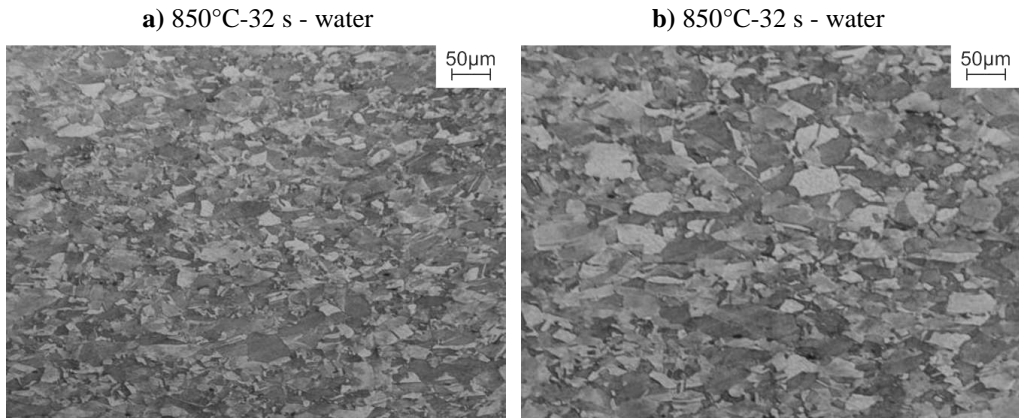
Figure 24. Fine, statically recrystallized austenite grains and large statically recovered grains of the 26Mn-3Si-3Al-Nb-Ti steel solution heat-treated from a temperature of 850°C after isothermal holding for 32 s of the specimen compressed with the true strain of 4x0.23 (a, b)

a) 850°C-32 s - water   **b)** 850°C-32 s - water
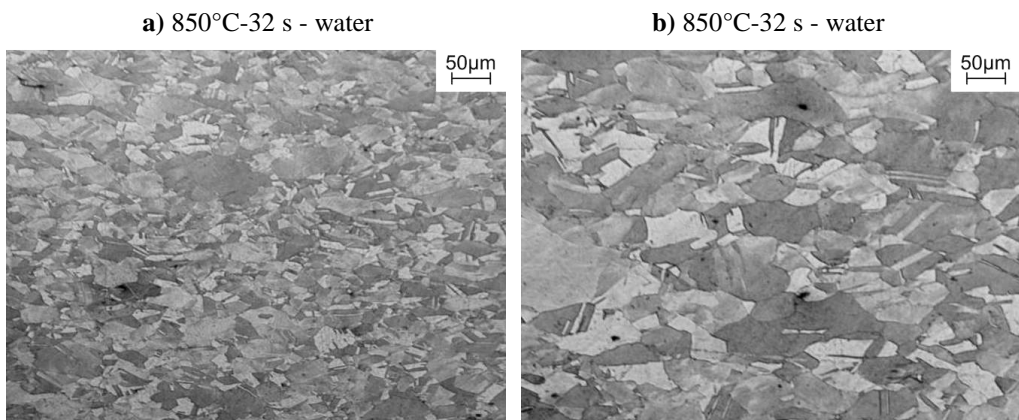
Figure 25. Fine, statically recrystallized austenite grains and large statically recovered grains of the 26Mn-3Si-3Al-Nb-Ti steel solution heat-treated from the temperature of 850°C after isothermal holding for 32 s of the specimen compressed with the true strain of 4x0.19 (a, b)

Further decrease of true strain to 0.19 causes that dynamic recovery is the process controlling work hardening in the whole temperature range of deformation (Fig. 15), at similar values of flow stress in comparison with the specimen deformed 4x0.23. However, the isothermal holding of the specimen for 32 s is to short to obtain a desired fraction of

recrystallized phase, which equals approximately 20% (Fig. 24a). Once again, numerous annealing twins can be observed in microstructure and fine statically recrystallized grains of γ phase are located mainly on boundaries of elongated statically recovered austenite grains (Fig. 24b).

4. Conclusions

Despite slight difference in chemical composition, brought mainly to concentration of Si and Al, elaborated steels show different microstructure in the initial state. Steel with higher Al concentration has stable microstructure of austenite with annealing twins, while steel with higher Si concentration consists of certain portion of ε martensite in form of plates. The differences in chemical composition don't have meaningful influence on behaviour of these steels in conditions of hot-working. Solutioning the steels do not change its phase composition but has essential effect on a grain size of austenite, which is fine-grained up to a temperature of about 1000°C.

Elaborated steels are characterized by relatively high values of flow stress, equal from 240 to 450 MPa, and values of ε_{max} deformation come from a range from 0.23 to 0.48, corresponding to maximum value of yield stress. Despite high value of ε_{max} at temperature of 850°C, initiation of dynamic recrystallization occurs already after true strain equal approximately 0.29, what creates possibility of refinement of microstructure. Dynamic recrystallization occurs more intensively in the steel containing 3%Al and 3%Si. It also results in faster course of removing the effects of hardening in the consequence of metadynamic recrystallization during isothermal holding of this steel in temperature of 900°C. Removal of strain hardening effects in steel 27Mn-4Si-2Al-Nb-Ti takes place mainly with participation of static recrystallization. The conditions of hot-working additionally influence phase state of investigated steels. Steel 26Mn-3Si-3Al-Nb-Ti keeps stable austenite microstructure independently from conditions of plastic deformation. Steel with initial bi-phase microstructure keeps a certain portion of martensite, yet dependant on conditions of hot-working. Grain size of γ phase as well as the state of internal stresses dependent on thermally activated mechanisms removing effects of strain hardening, have decisive influence on precipitation of the phase.

Determined half-times of recrystallization of austenite indicate that in the time of intervals between individual roll passes, partial recrystallization of γ phase should occur, contributing to achievement of fine-grained microstructure of steel. Faster course of metadynamic

recrystallization in 26Mn-3Si-3Al-Nb-Ti steel is probably caused by lower total concentration of Si and Mn, when comparing to 27Mn-4Si-2Al-Nb-Ti steel.

Taking advantage of dynamic recrystallization are confirmed by multi-stage compression results, in which lowering the flow stress in a range from 20 to 80 MPa dependent on a deformation temperature was observed and decreasing the critical strain ε_{max} to lower values. In case of applying the true strain 4x0.29, the refinement of the austenite microstructure during intervals between successive stages of deformation is caused by metadynamic recrystallization, whereas the fine-grained structure of the steel after the last deformation at a temperature of 850°C is a result of dynamic recrystallization. Further refinement of the microstructure can be obtained by isothermal holding of the steelss in a finishing hot-working temperature for about 16s. In case of applying the lower deformations 4x0.23 and 4x0.19 often used in finishing stages of hot-working, the process controlling work hardening is dynamic recovery and a deciding influence on a gradual grain refinement of microstructure has statical recrystallization occurring during intervals between successive stages of deformation and after its finish as well.

High-manganese austenite with a low SFE has a low tendency to dynamic recovery and forming a distinct cellular dislocation structure. Repeated recrystallization and corresponding grain refinement causes that the thermo-mechanically processed steel is characterized by uniform structure of γ phase without ε martensite plates. The fine-grained structure has influence on a phase composition of steel and should increase mechanical properties during subsequent cold plastic deformations.

Acknowledgements

References

1.   G. Frommeyer, U. Brüx, K. Brokmeier, R. Rablbauer, Development, microstructure and properties of advanced high-strength and supraductile light-weight steels based on Fe-Mn-Al-Si-(C),

Proceedings of the 6th International Conference on Processing and Manufacturing of Advanced Materials, Thermec'2009, Berlin, 2009, 162.

2. G. Frommeyer, O. Grässel, High strength TRIP/TWIP and superplastic steels: development, properties, application, La Revue de Metallurgie-CIT 10 (1998) 1299-1310.

3. G. Frommeyer, U. Brüx, P. Neumann, Supra-ductile and high-strength manganese-TRIP/TWIP steels for high energy absorption purposes, ISIJ International 43 (2003) 438-446.

4. O. Grässel, L. Krüger, G. Frommeyer, L.W. Meyer, High strength Fe-Mn-(Al, Si) TRIP/TWIP steels development – properties – application, International Journal of Plasticity 16 (2000) 1391-1409.

5. A. Saeed-Akbari, W. Bleck, U. Prahl, The study of grain size effect on the microstructure development and mechanical properties of a high-Mn austenitic steel, Proceedings of the 6th International Conference on Processing and Manufacturing of Advanced Materials, Thermec'2009, Berlin, 2009, 194.

6. K. Renard, H. Idrissi, S. Ryelandt, F. Delannay, D. Schryvers, P.J. Jacques, Strain-hardening mechanisms in Fe-Mn-C austenitic TWIP steels: Mechanical and micromechanical characterisation, Proceedings of the 6th International Conference on Processing and Manufacturing of Advanced Materials, Thermec'2009, Berlin, 2009, 72.

7. Y.G. Kim, J.M Han, J.S. Lee, Composition and temperature dependence of tensile properties of austenitic Fe-Mn-Al-C alloys, Materials Science and Engineering A 114 (1989) 51-59.

8. S. Allain, J.P. Chateau, O. Bouaziz, S. Migot, N. Guelton, Correlations between the calculated stacking fault energy and the plasticity mechanisms in Fe-Mn-C alloys, Materials Science and Engineering A 387-389 (2004) 158-162.

9. T. Bator, Z. Muskalski, S. Wiewiórkowska, J.W. Pilarczyk, Influence of the heat treatment on the mechanical properties and structure of TWIP steel in wires, Archives of Materials Science and Engineering 28 (2007) 337-340.

10. E. Mazancova, I. Schindler, K. Mazanec, Stacking fault energy analysis of the high manganese TWIP and TRIPLEX alloys, Hutnicke Listy 3 (2009) 55-58.

11. J. Kliber, T. Kursa, I. Schindler, The influence of hot rolling on mechanical properties of high-Mn TWIP steels, 3rd International Conference on Thermomechanical Processing of Steels, TMP'2008, (CD-ROM), Padua, 2008, s.1-12.

12. J. Kliber, T. Kursa, I. Schindler, Hot rolling of steel with TWIP effect, Metallurgist – Metallurgical News 8 (2008) 481-483.

13. S. Vercammen, B. Blanpain, B.C. De Cooman, P. Wollants, Mechanical behaviour of an austenitic Fe-30Mn-3Al-3Si and the importance of deformation twinning, Acta Materialia 52 (2004) 2005-2012.

14. A. Grajcar, W. Borek, The thermo-mechanical processing of high-manganese austenitic TWIP-type steels, Archives of Civil and Mechanical Engineering 8/4 (2008) 29-38.

15. L.A. Dobrzański, A. Grajcar, W. Borek, Influence of hot-working conditions on a structure of high-manganese austenitic steels, Journal of Achievements in Materials and Manufacturing Engineering 29/2 (2008) 139-142.

16. L.A. Dobrzański, A. Grajcar, W. Borek, Microstructure evolution and phase composition of high-manganese austenitic steels, Journal of Achievements in Materials and Manufacturing Engineering 31/2 (2008) 218-225.

17. A. Grajcar, M. Opiela, G. Fojt-Dymara, The influence of hot-working conditions on a structure of high-manganese steel, Archives of Civil and Mechanical Engineering 9/3 (2009) 49-58.

18. K.K. Jee, J.H. Han, W.Y. Jang, Measurement of volume fraction of ε martensite in Fe-Mn based alloys, Materials Science and Engineering A 378 (2004) 319-322.

19. G. Niewielski, Changes of structure and properties of austenitic steel caused by hot deformation, Scientific Books of the Silesian University of Technology 58, The Silesian University of Technology Publishers, Gliwice, 2000 (in Polish).

20. G. Niewielski, M. Hetmańczyk, D. Kuc, Influence of the initial grain size and deformation parameters on the mechanical properties during hot plastic deformation of austenitic steels, Materials Engineering 24/6 (2003) 795-798 (in Polish).

21. N. Cabanas, N. Akdut, J. Penning, B.C. De Cooman, High-temperature deformation properties of austenitic Fe-Mn alloys, Metallurgical and Materials Transactions A 37 (2006) 3305-3315.

22. A.S. Hamada, L.P. Karjalainen, M.C. Somani, The influence of aluminium on hot deformation behaviour and tensile properties of high-Mn TWIP steels, Materials Science and Engineering A 467 (2007) 114-124.

23. A.S. Hamada, L.P. Karjalainen, M.C. Somani, R.M. Ramadan, Deformation mechanisms in high-Al bearing high-Mn TWIP steels in hot compression and in tension at low temperatures, Materials Science Forum 550 (2007) 217-222.

24. M. Sabet, A. Zarei-Hanzaki, S. Khoddam, An investigation to the hot deformation behaviour of high-Mn TWIP steels, 3rd International Conference on Thermomechanical Processing of Steels, TMP'2008, (CD-ROM), Padua, 2008, s.1-7.

25. J. Kliber, K. Drozd, Stress-strain behaviour and softening in manganese TWIP steel tested in thermal-mechanical simulator, Hutnicke Listy 3 (2009) 31-36.

26. L.A. Dobrzański, A. Grajcar, W. Borek, Hot-working behaviour of high-manganese austenitic steels, Journal of Achievements in Materials and Manufacturing Engineering 31/1 (2008) 7-14.

27. L.A. Dobrzański, A. Grajcar, W. Borek, Microstructure evolution of high-manganese steel during the thermo-mechanical processing, Archives of Materials Science and Engineering 37 (2009) 69-76.

28. R. Kuziak, Modelling of structure changes and phase transformations occurring in thermo-mechanical processes of steel, Institute for Ferrous Metallurgy, Gliwice, 2005 (in Polish).

29. R. Kuziak, R. Kawalla, S. Waengler, Advanced high strength steels for automotive industry, Archives of Civil and Mechanical Engineering 8/2 (2008) 103-117.

30. H. Takechi, Application of IF based sheet steels in Japan, Proceedings of the International Conference on the Processing, Microstructure and Properties of IF Steels, Pittsburgh, 2000, 1-12.

31. J. Adamczyk, A. Grajcar, Heat treatment and mechanical properties of low-carbon steel with dual-phase microstructure, Journal of Achievements in Materials and Manufacturing Engineering 22/1 (2007) 13-20.

32. A.K. Lis, B. Gajda, Modelling of the DP and TRIP microstructure in the CMnAlSi automotive steel, Journal of Achievements in Materials and Manufacturing Engineering 15 (2006) 127-134.

33. A. Grajcar, Hot-working in the $\gamma+\alpha$ region of TRIP-aided microalloyed steel, Archives of Materials Science and Engineering 28/12 (2007) 743-750.

34. B. Gajda, A.K. Lis, Thermal processing of CMnAlSi steel at $(\alpha+\gamma)$ temperature range, Journal of Achievements in Materials and Manufacturing Engineering 18 (2006) 355-358.

35. E. Doege, S. Kulp, Ch. Sunderkötter, Properties and application of TRIP-steel in sheet metal forming, Steel Research 73 (2002) 303-308.

36. S. Ganesh, S. Raman, K.A. Padmanabhan, Tensil deformation-induced martensitic transformation in AISI 304LN austenitic stainless steel, Journal of Materials Science Letters 13 (1994) 389-392.

37. S. Allain, J.P. Chateau, O. Bouaziz, S. Migot, N. Guelton, Correlations between the calculated stacking fault energy and the plasticity mechanisms in Fe-Mn-C alloys", Materials Science and Engineering A 387-389 (2004) 158-162.

38. J. Adamczyk, Theoretical Physical Metallurgy, The Silesian University of Technology Publishers, Gliwice, 2002, (in Polish).

39. A.D. Paepe, J.C. Herman, Improved deep drawability of IF-steels by the ferrite rolling practice, Proceedings of the 37th Mechanical Working and Steel Processing Conference, Baltimore, 1999, 951-962.